Profile of a decaying crystalline cone

Navot Israeli* and Daniel Kandel†
Department of Physics of Complex Systems, Weizmann Institute of Science, Rehovot 76100, Israel
(Received 4 May 1999)

The decay of a crystalline cone below the roughening transition is studied. We consider local mass transport through surface diffusion, focusing on the two cases of diffusion limited and attachment-detachment limited step kinetics. In both cases, we describe the decay kinetics in terms of step-flow models. Numerical simulations of the models indicate that in the attachment-detachment limited case the system undergoes a step-bunching instability if the repulsive interactions between steps are weak. Such an instability does not occur in the diffusion limited case. In stable cases the height profile, $h(r,t)$, is flat at radii $r<R(t)\sim t^{1/4}$. Outside this flat region the height profile obeys the scaling scenario $\partial h/\partial r=\mathcal{F}(rt^{-1/4})$. A scaling ansatz for the time-dependent profile of the cone yields analytical values for the scaling exponents and a differential equation for the scaling function. In the long-time limit, this equation provides an exact description of the discrete step dynamics. It admits a family of solutions and the mechanism responsible for the selection of a unique scaling function is discussed in detail. Finally, we generalize the model and consider permeable steps by allowing direct adatom hops between neighboring terraces. We argue that step permeability does not change the scaling behavior of the system, and its only effect is a renormalization of some of the parameters. [S0163-1829(99)04332-5]

I. INTRODUCTION

The properties of crystalline nanostructures are of considerable interest because of the technological importance of nanostructures in fabrication of electronic devices. Kinetic properties of nanostructures attracted particular attention, since in many cases nanostructures are thermodynamically unstable and tend to decay with time. Such decay processes have been studied both theoretically and experimentally.

Considerable effort was devoted to the study of periodic structures. The decay of one- and two-dimensional gratings was studied extensively. The emerging experimental picture[1–4] is that below the roughening temperature these structures decay in a shape-preserving manner. Macroscopic facets are observed at the maxima and minima of the gratings. Although these systems are out of equilibrium, the appearance of facets is a manifestation of the cusp singularity of the surface free energy at the high-symmetry crystalline orientation.

There are basically two theoretical approaches to the problem of surface evolution in general and nanostructure decay in particular. On the one hand, there are phenomenological models which treat the crystal surface as a continuous medium.[5–10] The evolution of the surface is then driven by the tendency of the system to lower its free energy (given in terms of continuous spatial variables). The advantage of such models is that they are relatively simple and can sometimes lead to analytical predictions of surface evolution. However, these models ignore the discrete nature of surface steps, which may become important below the roughening transition. In addition, most of them rely on assumptions of small surface slope and/or surface curvature (with the exception of Ref. 8), and are unable to properly treat the behavior of the macroscopic facets observed experimentally.

On the other hand, there are models which treat surface evolution on a smaller scale. Among these are microscopic models,[11–14] where the basic degrees of freedom are individual atoms, and step-flow models.[10,15–18] These models are usually solved numerically, and provide results which can be directly related to the microscopic dynamics. However, in most cases, it is difficult to understand the behavior of the system on larger length scales on the basis of these results.

Research efforts were also directed towards isolated surface structures. The decay of isolated step bunches, islands, or hills was studied both experimentally[19,20] and theoretically.[21–23] Here too there is an apparent gap between the microscopic and macroscopic theoretical approaches.

In this work we attempt to bridge this gap in the case of a simple surface structure, i.e., an infinite crystalline cone. We give a complete account of the surface dynamics based on a step-flow model, and then derive a continuum model which gives a very accurate description of the evolution of the cone and becomes exact in the long-time limit. We do not make any assumptions of small slope or small surface curvature.

The crystalline cone consists of an infinite number of circular concentric steps. A similar system was studied by Rettori and Villain,[15] who considered the decay of bidirectional surface modulations. Their results are relevant in the case of small amplitude modulations when the profile peaks and valleys affect each other. Our work addresses the opposite situation when a single peak can be considered as an isolated structure and in this sense is complimentary to theirs.

Below the roughening transition, atomic steps have a finite free energy. Their existence on the surface strongly affects its morphological evolution. In many cases, one can ignore the formation of islands and voids on the surface and consider only adatom diffusion and attachment and detachment processes to and from step edges. The decay of a nanostructure is then dominated by the motion of steps. In order to describe the decay process mathematically, one has to solve the diffusion equation for adatoms on the terraces between the steps, with boundary conditions at the step edges, in the spirit of the Burton-Cabrera-Frank model.[24] If the geometry of the nanostructure is simple, this procedure leads to

 ©1999 The American Physical Society

a set of coupled equations of motion for the steps. Our goal in the present work is to construct and solve these equations of motion for the simple case of an infinite crystalline cone. A partial account of this work is found in Ref. 25. The kinetic step model for the cone is derived in Sec. II. In Sec. III we carry out numerical simulations of the model and examine the evolution of surface morphology under various conditions.

Previous experimental and theoretical research on decay of nanostructures has demonstrated that in most cases the surface reaches a scaling state where the typical length scale depends on time algebraically. Our simulations show that the cone profile also exhibits such a scaling behavior. In Sec. IV we show analytically that the step-flow model admits such solutions. We calculate the scaling exponents and derive a continuum equation for the scaling function. The properties of the scaling function are analyzed in Secs. V and VI.

It has been suggested that in some materials steps may be permeable to flow of atoms; i.e., atoms can hop between neighboring terraces without attaching to the step which separates them. In Sec. VII we discuss the consequences of step permeability on the decay of an infinite cone, and show that permeability does not change the qualitative behavior of the system.

II. STEP-FLOW MODEL OF A CRYSTALLINE CONE

We now consider a crystalline surface which consists of flat terraces, parallel to a high-symmetry plane of the crystal and separated by atomic steps. Islands and voids are ignored. The evolution of such systems of steps was treated long ago by Burton, Cabrera, and Frank[24] (BCF). The BCF theory assumes that mass transfer between terraces is governed by diffusion of adatoms on the terraces. These atoms are emitted and absorbed at step edges, which according to BCF act as perfect sinks and sources. This last assumption, however, is valid only when adatom diffusion is the rate limiting process. Modifications of the BCF model account for the finite rate of adatom attachment-detachment processes at step edges. The BCF model was also generalized to include elastic and entropic interactions between steps (see, for example, Refs. 10 and 26). In this section we construct such a generalized BCF model for the morphological evolution of a conic hill on a crystal surface.

Consider the surface of an infinite crystalline cone, which consists of circular concentric steps of radii $r_i(t)$, separated by flat terraces (Fig. 1). The index i grows in the direction away from the center of the cone. These steps may absorb or emit atoms, which then diffuse across the neighboring terraces with a diffusion constant D_s. Assuming no deposition of new material, no evaporation, and no transport through the bulk, the adatom concentration $C_i(\vec{r})$ on the ith terrace satisfies the diffusion equation

$$D_s \nabla^2 C_i(\vec{r}) = \frac{\partial C_i(\vec{r})}{\partial t},$$

where $\vec{r}$ is a two-dimensional vector parallel to the high-symmetry terraces. In most situations, the time scale associated with step motion is much larger than the time scale of surface diffusion. One can therefore assume that the adatom

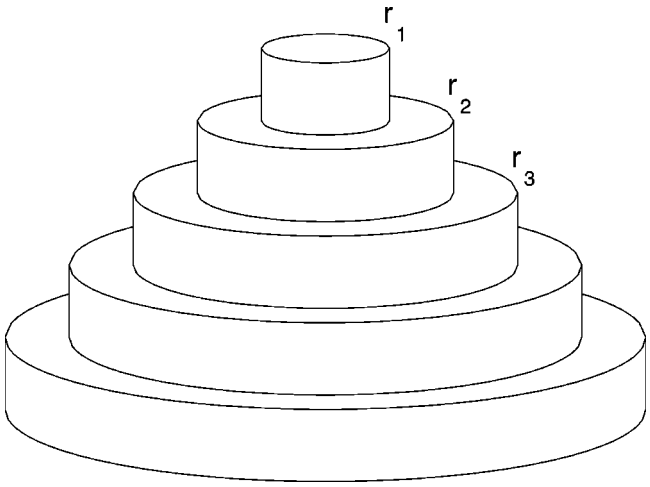

FIG. 1. Illustration of the step configuration in a crystalline cone. The step height is exaggerated.

diffusion field is always in a steady state; i.e., for any step configuration, the diffusion field reaches a steady state before the steps move significantly. Within this quasistatic approximation, the right-hand side of the diffusion equation can be neglected. Using the radial symmetry of the cone, we can write the static diffusion equation in polar coordinates as

$$\frac{\partial^2 C_i(r)}{\partial r^2} + \frac{1}{r}\frac{\partial C_i(r)}{\partial r} = 0. \tag{1}$$

The general solution of this equation is

$$C_i(r) = A_i \ln r + B_i. \tag{2}$$

The coefficients A_i and B_i are determined by the boundary conditions at the step edges. To define these conditions, we assume that the flux of atoms at the two step edges bounding the ith terrace is determined by first-order kinetics, characterized by an attachment-detachment rate coefficient k:

$$D_s \left.\frac{\partial C_i}{\partial r}\right|_{r_i} = k(C_i|_{r_i} - C_i^{\mathrm{eq}}),$$

$$-D_s \left.\frac{\partial C_i}{\partial r}\right|_{r_{i+1}} = k(C_i|_{r_{i+1}} - C_{i+1}^{\mathrm{eq}}), \tag{3}$$

where C_i^{eq} is the equilibrium concentration of atoms on the terrace adjacent to the ith step. Using these boundary conditions, we find that the constants A_i are given by

$$A_i = \frac{C_i^{\mathrm{eq}} - C_{i+1}^{\mathrm{eq}}}{\ln r_i - \ln r_{i+1} - \frac{D_s}{k}\left(\frac{1}{r_i} + \frac{1}{r_{i+1}}\right)}. \tag{4}$$

Employing mass conservation at the step, we obtain the step velocity,

$$\frac{dr_i}{dt} = \Omega D_s \left.\left(\frac{\partial C_i}{\partial r} - \frac{\partial C_{i-1}}{\partial r}\right)\right|_{r_i} = \Omega D_s \frac{A_i - A_{i-1}}{r_i}, \tag{5}$$

where Ω is the atomic area of the solid.

In order to complete the solution of the diffusion problem, we have to determine the equilibrium adatom concentration at step edges. This concentration depends on the local step curvature and on the radii of neighboring steps. According to the Gibbs-Thomson relation, $C_i^{\rm eq}$ is given by

$$C_i^{\rm eq}=\overline{C}^{\rm eq}\exp\frac{\mu_i}{T}\approx\overline{C}^{\rm eq}\left(1+\frac{\mu_i}{T}\right), \tag{6}$$

in units where the Boltzmann constant is equal to 1. Here μ_i is the chemical potential associated with the addition of an atom to the solid at the ith step, T is the temperature, and $\overline{C}^{\rm eq}$ is the adatom equilibrium concentration at the edge of a straight isolated step. To evaluate the step chemical potential, μ_i, we take into account the step line tension, Γ, and a repulsive interaction between nearest-neighbor steps. The magnitude of this interaction is inversely proportional to the square of the distance between the steps at large distances. Such a dependence is consistent with entropic as well as elastic[27,28] interactions between straight steps. We follow Ref. 16 and take the interaction energy between step $i+1$ and an atomic segment of the ith step to be

$$U(r_i,r_{i+1})=\frac{G\sqrt{\Omega}r_{i+1}}{(r_i+r_{i+1})(r_{i+1}-r_i)^2}, \tag{7}$$

where G is the interaction strength. The chemical potential of the ith step is then given by

$$\mu_i=\frac{\Omega\Gamma}{r_i}+\sqrt{\Omega}\,\frac{\partial[U(r_i,r_{i+1})+U(r_i,r_{i-1})]}{\partial r_i}. \tag{8}$$

This equation applies also to the chemical potential of the first step if we set $r_0=0$.

As we show below, in the long-time limit the distance between steps is small compared with the step radius. In this limit we can approximate the step chemical potential by

$$\mu_i=\frac{\Omega\Gamma}{r_i}+\Omega G\left(\frac{2r_{i+1}}{r_{i+1}+r_i}\,\frac{1}{(r_{i+1}-r_i)^3}-\frac{2r_{i-1}}{r_i+r_{i-1}}\,\frac{1}{(r_i-r_{i-1})^3}\right). \tag{9}$$

This approximation simplifies the algebra considerably, and we verified that it does not affect the analytical and numerical results described below.

We are now ready to write down the step equations of motion using Eqs. (4), (5), and the Gibbs-Thomson relation (6). It is convenient to use dimensionless radii, ρ_i, and dimensionless time τ:

$$\rho_i=\frac{T}{\Omega\Gamma}r_i,$$

$$\tau=D_s\overline{C}^{\rm eq}\Omega\left(\frac{T}{\Omega\Gamma}\right)^2\left(1+\frac{D_sT}{k\Omega\Gamma}\right)^{-1}t.$$

In terms of these variables, the equations of motion take the form

$$\dot{\rho}_i\equiv\frac{d\rho_i}{d\tau}=\frac{a_i-a_{i-1}}{\rho_i},$$

with

$$a_i=\frac{\xi_i-\xi_{i+1}}{(1-q)\ln\dfrac{\rho_i}{\rho_{i+1}}-q\left(\dfrac{1}{\rho_i}+\dfrac{1}{\rho_{i+1}}\right)},$$

$$\xi_i=\frac{1}{\rho_i}+g\left(\frac{2\rho_{i+1}}{\rho_{i+1}+\rho_i}\cdot\frac{1}{(\rho_{i+1}-\rho_i)^3}-\frac{2\rho_{i-1}}{\rho_i+\rho_{i-1}}\cdot\frac{1}{(\rho_i-\rho_{i-1})^3}\right). \tag{10}$$

Equations (10) depend on two parameters: $g=T^2G/(\Omega^2\Gamma^3)$ measures the strength of step-step interactions G relative to the line tension Γ, while the parameter $q=[1+k\Omega\Gamma/(D_sT)]^{-1}$ determines the rate limiting process in the system. When $q\to1$, diffusion across terraces is fast and the rate limiting process is attachment and detachment of adatoms to and from steps. On the other hand, when $q\to0$, the steps act as perfect sinks and the rate limiting process is diffusion across terraces.

III. RESULTS OF SIMULATIONS

We integrated Eqs. (10) numerically both in the case of diffusion limited kinetics (DL) and in the case of attachment-detachment limited kinetics (ADL). The initial configuration was a uniform step train. In principle, the initial step separation is a parameter of the model. However, for any value of this parameter one can change the units of length and time and get the same equations of motion with initial step separation of unity and different values of the parameters g and q. Thus it is sufficient to consider an initial step separation of unity.

When the repulsive interactions between steps are weak (i.e., g is small), there is a striking difference between the dynamics in the DL and ADL limits. In the ADL case the system becomes unstable towards step bunching, whereas in the DL case there is no such instability. However, when g is large enough the instability disappears even in the ADL case. Let us first discuss situations where the step bunching instability does not occur. Figure 2 shows the time evolution of the system in the ADL and the DL cases with a relatively large value of g. Each line in the figures describes the evolution of the radius of one step. We note that the innermost step shrinks while the other steps expand and absorb the atoms emitted by the first step. When the innermost step disappears, the next step starts shrinking, and so on. Our observations indicate that the time at which the nth step disappears, τ_n, grows with n as $\tau_n\sim n^4$. This process results in a propagating front, which leaves a growing plateau or a facet at the center of the cone. At large times, the (dimensionless) position of this front behaves as $\rho_{\rm front}(\tau)\sim\tau^{1/4}$. This is shown by the dashed lines in Fig. 2.

This power law is an indication of a much more general and interesting phenomenon. It turns out that at large times, not only the front position but also the positions of minimal

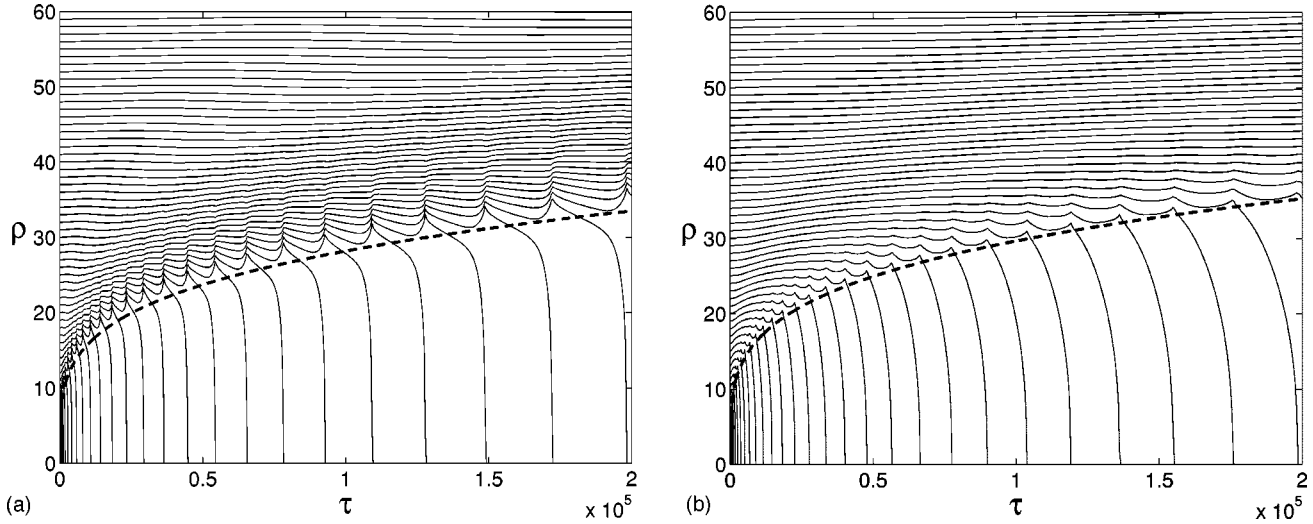

FIG. 2. Time evolution of the step radii in the (a) ADL and (b) DL cases with $g=0.01$. The radius of the facet edge can be fitted by a $\tau^{1/4}$ power law (dashed lines).

and maximal step densities scale as $\tau^{1/4}$. In fact, the step density $D(\rho,\tau)$, defined as the inverse step separation, obeys the following scaling scenario: There exist scaling exponents α, β, and γ, which define the scaled variables $x\equiv\rho\tau^{-\beta/\gamma}$ and $\theta\equiv\tau^{1/\gamma}$. In terms of these variables

$$D(\rho,\tau)=\theta^{\alpha}F(x,\theta), \tag{11}$$

where the scaling function F is a *periodic* function of θ with some period θ_0. Our ansatz is somewhat weaker than standard scaling hypotheses, which would assume the scaling function F is independent of θ. We introduce this periodic dependence because our simulations strongly indicate a periodic behavior, generated by the motion of the first step (see Fig. 2). Thus the disappearance time of step n is $\tau_n=(n\theta_0)^{\gamma}$. An immediate consequence of the scaling ansatz is that if we define $\theta=\overline{\theta}+n\theta_0$ with $0\leq\overline{\theta}<\theta_0$, and plot $\theta^{-\alpha}D(\rho,\tau)$ against x, all the data with different values of n and the *same* value of $\overline{\theta}$ collapse onto a single curve, $F(x,\overline{\theta})$.

To verify that our system obeys this scaling ansatz, we define the step density at a discrete set of points in the middle of the terraces:

$$D\left(\frac{\rho_i(\tau)+\rho_{i+1}(\tau)}{2},\tau\right)=\frac{1}{\rho_{i+1}(\tau)-\rho_i(\tau)}. \tag{12}$$

Figure 3 shows plots of $D(\rho,\tau)$ as a function of $x=\rho\tau^{-1/4}$ for a fixed value of $\overline{\theta}$ and six different values of n in the ADL and the DL cases. The excellent data collapse shows that our scaling ansatz indeed holds with $\alpha=0$, $\beta=1$, and $\gamma=4$ in both cases.

We now turn to discuss effects of interactions between steps. As shown above, the behavior of the cone in the ADL

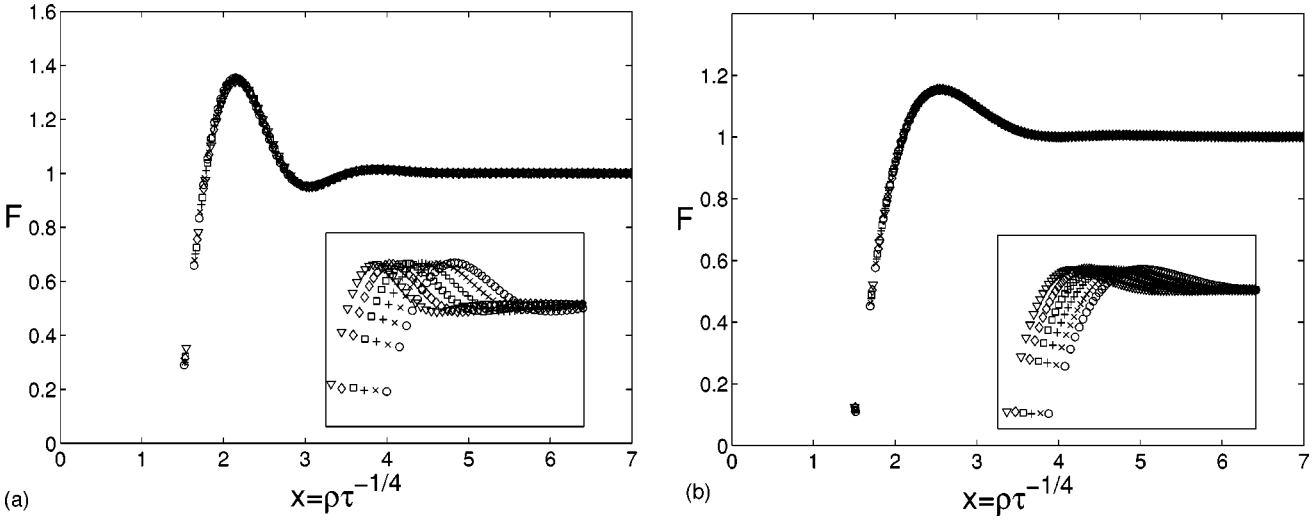

FIG. 3. Data collapse of the density function in the (a) ADL and (b) DL cases with $g=0.01$. The values of the scaling exponents used here are $\alpha=0$, $\beta=1$, and $\gamma=4$. These figures show density functions with six different values of n and the same value of $\overline{\theta}$, as a function of $x=\rho\tau^{-1/4}$. Different symbols correspond to different values of n. The unscaled data are shown in the insets.

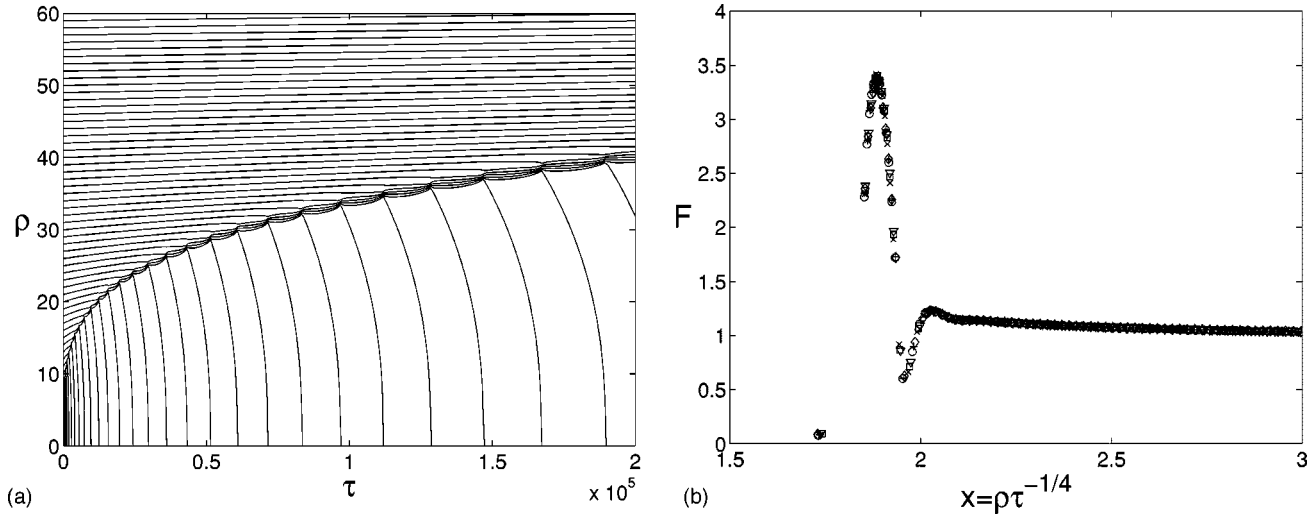

FIG. 4. (a) Time evolution of the step radii in the DL case with $g=10^{-6}$. (b) Data collapse of the density function in the same system. Different symbols correspond to different times.

and the DL limits is very similar when the repulsion between steps is strong. We have already mentioned that when the repulsion is weak, the behavior of the system in the DL limit is very different from its behavior in the ADL case. This is not surprising, since linear stability analysis (see Appendix A) of the two cases in the absence of step-step interactions predicts that the ADL case is unstable towards step bunching while the DL case is marginal. In intermediate cases ($0<q<1$) the system is unstable when the interactions are sufficiently weak.

Figure 4 shows the time evolution and the data collapse of the density function in the DL case when step-step interactions are weak. As one can see, the behavior of the cone is qualitatively similar to the large g example [Fig. 2(b)] and the scaling ansatz still holds. Quantitatively, the step density near the facet edge is much higher for small values of g. Also the dependence of the scaling function on scaled time within a collapse period is much more pronounced when the interactions are weak.

The dependence of step kinetics on the strength of the interactions is much more complicated in the ADL case. Figure 5 shows the evolution and, when possible, the scaled density function of a series of ADL systems which differ in the value of g. The two quantitative observations we made in the DL case also hold here: The high step-density region near the front becomes more dense, and the time dependence of the scaling function becomes more pronounced as the value of g is reduced [Figs. 5(a)–5(d)]. In addition, we noted that the approach of the system towards the scaling state is slower. Adjacent to the dense region at the edge of the facet is another region of very low density of steps. This region becomes less dense as the value of g is reduced. Below a critical value, g_c, of the interaction parameter, a few steps between the low-density region and the facet edge form a bunch. At this stage the scaling ansatz breaks down. The system no longer exhibits a simple periodic nature, which results from the collapse of single steps, one at a time. Instead, it seems to adopt a complicated almost periodic pattern which involves the collapse of many steps in each period [Fig. 5(e)]. Hints for this periodicity changes are already present in Figs. 5(a) and 5(c), where the steps crossing the low-density region follow a threefold periodicity. If the value of g is further reduced, bunches of steps collapse together, and finally the whole system becomes unstable toward step bunching [Fig. 5(f)]. Neighboring steps merge and form a bunch, which in turn merges with another bunch, and so on. Step bunches rather than isolated steps become the dynamic objects in the system.

IV. SCALING ANALYSIS AND THE CONTINUUM MODEL

The above results suggest that when the step-bunching instability does not occur, the time evolution of the system can be described by a step-density function, which is continuous in both position and time variables. In this section we derive such a continuum model by carrying out a scaling analysis. We obtain an equation which governs the scaling function and evaluate the scaling exponents analytically.

Motivated by the simulation results, we assume that at long times the scaling ansatz, Eq. (11), holds. This, together with conservation of the total volume of the system, already determines the two scaling exponents α and β. First, we derive a relation between these scaling exponents by considering the height profile $h(\rho,\tau)$. Assuming steps of unit height, the height difference between two points on the surface is given by the number of steps between them. The continuous analog of this statement can be used to derive the following relation between the height profile and the step density:

$$h(\rho,\tau)=h_0(\tau)-\int_0^{\rho}D(\rho',\tau)d\rho', \tag{13}$$

where $h_0(\tau)$ is the height at the origin. Far enough (in the limit $\rho\to\infty$), $h(\rho,\tau)$ does not change with time. Calculating the height change at infinity using Eq. (13), we find

$$h_0(\tau)-h_0(0)-\tau^{(\alpha+\beta)/\gamma}\int_0^{\infty}[F(x,\theta)-F(\infty,0)]dx=0, \tag{14}$$

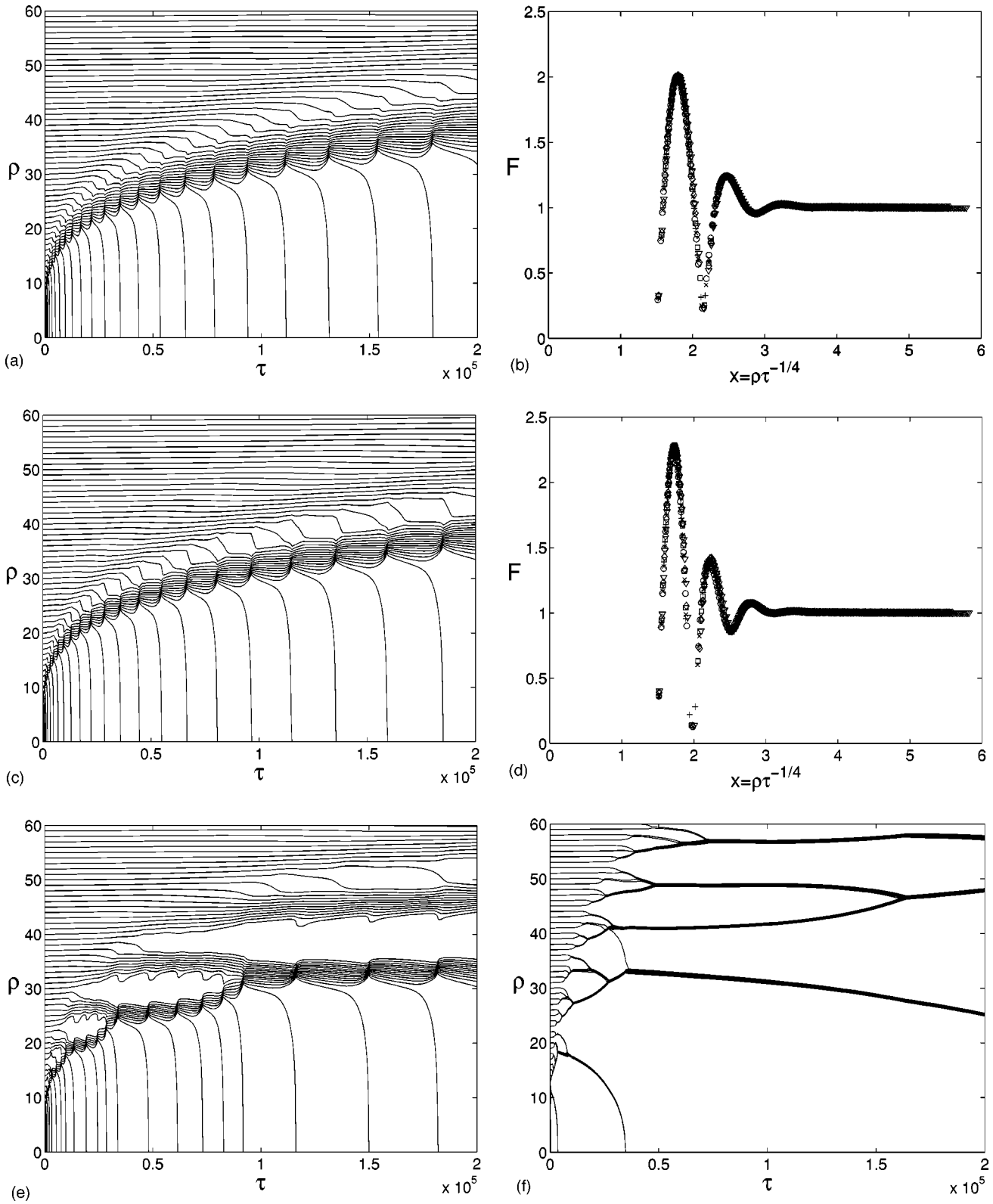

FIG. 5. Time evolution and scaled density functions of ADL systems with different interaction strengths. (a) and (b) $g=10^{-3}$, (c) and (d) $g=5\times10^{-4}$, (e) $g=2.5\times10^{-4}$, and (f) $g=10^{-6}$.

where we have changed the integration variable and used the definition [Eq. (11)] of the scaling function F. On the other hand, $h_0(0)-h_0(\tau_n)=n$ because τ_n is the time of disappearance of the nth step. γ satisfies the relation $\tau_n\sim n^{\gamma}$, and therefore we have $h_0(0)-h_0(\tau_n)\sim\tau_n^{1/\gamma}$. This and the $\tau^{(\alpha+\beta)/\gamma}$ dependence in Eq. (14) lead to the relation $\alpha+\beta=1$.

In addition, conservation of the total volume of the system, $\mathcal{V}$, implies that

$$\mathcal{V}=2\pi\int_0^{\infty}\rho h(\rho,\tau)d\rho \tag{15}$$

is independent of τ. Integration by parts of the derivative of this integral with respect to τ yields the following equation:

$$\int_0^\infty \rho^2 \frac{\partial D(\rho,\tau)}{\partial \tau} d\rho = 0. \tag{16}$$

Evaluating this integral in terms of the function F and the scaled variables x and θ, we obtain the equation

$$\int_0^\infty x^2 \left[\frac{\alpha F(x,\theta)}{\theta} + \frac{\partial F(x,\theta)}{\partial \theta} \right] dx = 0. \tag{17}$$

This can be satisfied for all θ only if $\alpha = 0$, since F is a periodic function of θ. Combining this result with the previously obtained relation $\alpha + \beta = 1$, we conclude that

$$\alpha = 0, \quad \beta = 1. \tag{18}$$

Thus, γ is the only nontrivial scaling exponent in the model. To evaluate γ and the scaling function F, we continue with the equation for the full time derivative of the step density D:

$$\frac{dD}{d\tau} = \frac{\partial D}{\partial \tau} + \frac{\partial D}{\partial \rho} \frac{d\rho}{d\tau}. \tag{19}$$

Equation (19) can be evaluated in the middle of the terrace between two steps (i.e., at $\rho = (\rho_i + \rho_{i+1})/2$). The left-hand side of Eq. (19) is calculated by taking the time derivative of Eq. (12): $dD/d\tau = -D^2(\dot{\rho}_{i+1} - \dot{\rho}_i)$. This, together with the fact that $d\rho/d\tau = (\dot{\rho}_i + \dot{\rho}_{i+1})/2$, leads to the relation

$$\frac{\partial D}{\partial \rho} \frac{\dot{\rho}_{i+1} + \dot{\rho}_i}{2} + \frac{\partial D}{\partial \tau} + D^2(\dot{\rho}_{i+1} - \dot{\rho}_i) = 0. \tag{20}$$

Now we change variables to θ and $x_i \equiv \rho_i \theta^{-1}$ (since $\beta = 1$), and transform Eq. (20) into an equation for the scaling function F:

$$\frac{\partial F}{\partial x} \left(\theta^{\gamma-1} \frac{\dot{\rho}_{i+1} + \dot{\rho}_i}{2} - \frac{x}{\gamma} \right) + \frac{\theta}{\gamma} \frac{\partial F}{\partial \theta} + F^2 \theta^\gamma (\dot{\rho}_{i+1} - \dot{\rho}_i) = 0. \tag{21}$$

The step velocities $\dot{\rho}_i$ and $\dot{\rho}_{i+1}$ can also be expressed in terms of the x_i's, but we defer this algebraic manipulation to a later stage.

Our next goal is to take a continuum limit of Eq. (21) in the variable $x = (x_{i+1} + x_i)/2$. Such a continuum limit becomes exact in the long-time limit. To see this, let us rewrite Eq. (12) in terms of x_i's, θ, and F:

$$x_{i+1} - x_i = \frac{\theta^{-1}}{F((x_{i+1} + x_i)/2, \theta)}. \tag{22}$$

According to this equation, the difference between successive x_i's is of order θ^{-1} wherever F does not vanish. In the large θ (long-time) limit, these differences become vanishingly small. This justifies the continuum limit in the variable x.

In practice, we take the continuum limit in the following way. We evaluate the function F at the position $(x_{i+k} + x_{i+k+1})/2$ by using its Taylor expansion

$$F\left(\frac{x_{i+k} + x_{i+k+1}}{2}, \theta \right) \equiv \frac{\theta^{-1}}{x_{i+k+1} - x_{i+k}} = \sum_{n=0}^\infty \frac{1}{n!} \frac{\partial^n F(x,\theta)}{\partial x^n} \times \left(\frac{x_{i+k} + x_{i+k+1}}{2} - x \right)^n. \tag{23}$$

As long as k is finite, the difference $x_{i+k} - x$ is small in the long-time limit. It is therefore useful to expand x_{i+k} around x,

$$x_{i+k} = x + \sum_{n=1}^\infty \phi_{kn} \theta^{-n}, \tag{24}$$

and insert this expansion into Eq. (23). The resulting equation is expanded as a power series in θ^{-1}. By requiring that the equation be obeyed to all orders in θ^{-1}, we can calculate the coefficients ϕ_{kn} for any desired k and n. These coefficients will involve the function F and its derivatives with respect to x, which are all periodic functions of θ.

Next, we express the velocities $\dot{\rho}_i$ and $\dot{\rho}_{i+1}$ in terms of the scaled radii $x_{i-2}, x_{i-1}, \ldots, x_{i+3}$ using Eq. (10) and the transformation to scaled variables. We then use Eq. (24) to expand the velocities in powers of θ^{-1}. The result of this expansion is

$$\begin{aligned} \dot{\rho}_{i+1} + \dot{\rho}_i &= \theta^{-3}[\mathcal{A} + O(\theta^{-1})], \\ \dot{\rho}_{i+1} - \dot{\rho}_i &= \theta^{-4}[\mathcal{B} + O(\theta^{-1})]. \end{aligned} \tag{25}$$

$\mathcal{A}$ and $\mathcal{B}$ are known expressions involving F, F', F'', F''', F'''', where the primes denote partial derivatives with respect to x. The full expressions are given in Appendix B. The existence of derivatives up to fourth order in this equation is a consequence of the fact that each step ''interacts'' with four other steps (two on each side) through the equations of motion (10). Inserting Eqs. (25) into Eq. (21), we obtain the following differential equation for F:

$$-F' \frac{x}{\gamma} + \theta^{\gamma-4} \left(F' \frac{\mathcal{A}}{2} + F^2 \mathcal{B} \right) + \frac{\theta}{\gamma} \frac{\partial F}{\partial \theta} + O(\theta^{\gamma-5}) = 0. \tag{26}$$

Consider Eq. (26) at large θ. Our expansion in the small parameter θ^{-1} is valid only at values of x where F does not diverge or vanish (see above). Therefore, the first term in Eq. (26) is $O(1)$. This term has to be canceled by the second term if we require F to satisfy a single differential equation. Hence, we must have

$$\gamma = 4. \tag{27}$$

The fourth term vanishes as $\theta \to \infty$ since $\gamma - 5 < 0$, and the third term must vanish as well. Therefore, in the large θ limit, F is only a function of x, and we are left with an ordinary differential equation for F:

$$F' \left(\frac{\mathcal{A}}{2} - \frac{x}{4} \right) + F^2 \mathcal{B} = 0. \tag{28}$$

The detailed form of this equation in the DL and ADL cases is also given in Appendix B.

Let us emphasize several important properties of our scaling analysis. First, the values of the scaling exponents we calculated ($\alpha=0$, $\beta=1$, and $\gamma=4$) are consistent with the results of numerical simulations (see above). Second, our continuum model is valid for arbitrarily large surface curvature and slope (unlike other treatments[10,15]). Moreover, since our model is an expansion in the truly small parameter θ^{-1} [see Eq. (22)] it becomes *exact* in the large θ (long-time) limit. Finally, note that in going to the continuum limit we lost the periodic dependence of F on θ. This periodicity is generated by the first step, which follows a unique equation of motion. We did not incorporate this unique behavior into the continuum model and therefore should not be surprised that this information is lost.

As we emphasized, our continuum model is an exact representation of the original discrete system. For this reason it is interesting to compare it with other continuum models, which do not emerge as limits of discrete systems of steps. Many authors use the continuity equation

$$\frac{\partial h}{\partial t}+\nabla\vec{J}=0 \tag{29}$$

to account for the surface evolution. Here h is the surface height and $\vec{J}$ is the current density of diffusing adatoms. This equation is of course correct and reduces the problem to calculating $\vec{J}$. It is widely assumed[8,10] that $\vec{J}$ is proportional to the gradient of the surface chemical potential μ, as expected in diffusive systems. In the case of attachment-detachment limited systems it was suggested by Nozières[29] that the chemical potential gradient should be divided by the profile slope. Our model is consistent with the first picture in the DL case and with the second in the ADL case.

To show this, we take the gradient of Eq. (29). This leads to

$$\frac{\partial\vec{D}}{\partial t}\propto\nabla\nabla\cdot\vec{J}, \tag{30}$$

where $-\vec{D}$ is the gradient of the profile. We now return to Eq. (28) and transform it back to an equation for the step density $D(\rho,\tau)$. Remembering that the term $-xF'/4$ in Eq. (28) arises from the time derivative of D, we find that in the general case we can write

$$\frac{\partial D}{\partial\tau}+\frac{\partial}{\partial\rho}\left[\frac{1}{\rho}\frac{\partial}{\partial\rho}\left(\frac{\rho}{1-q+2qD}\cdot\frac{\partial\mu}{\partial\rho}\right)\right]=0 \tag{31}$$

with

$$\mu=\frac{1}{\rho}+g\left(\frac{D^2}{\rho}+3D\frac{\partial D}{\partial\rho}\right).$$

Equation (31) is nothing but the radial component of Eq. (30) written in terms of the dimensionless variables ρ and τ with

$$J=\frac{1}{1-q+2qD}\frac{\partial\mu}{\partial\rho}. \tag{32}$$

Therefore in the DL case ($q=0$) the adatom current is indeed proportional to the chemical potential gradient. In the ADL case ($q=1$) the chemical potential gradient is divided by the local step density as suggested by Nozières. In addition, we note that in the limit $\rho\to\infty$ (where the steps are nearly straight), our chemical potential [Eq. (31)] becomes identical to the chemical potential of Ref. 8.

V. PROPERTIES OF THE SCALING FUNCTION

In this section we use Eq. (28) to study properties of the scaling function F. We also discuss the boundary conditions necessary to solve Eq. (28). We begin by noting that according to the numerical simulations of the step model, there is a growing plateau or facet at the top of the cone. Our numerical solutions for the scaling function indicate that all physical solutions indeed have such a special point, which can be identified as the facet edge. Let us examine the behavior of the step density on the facet and at its edge. At any given time there is only one single step on the facet (the first step during its collapse towards the origin). We have seen that the size of the facet grows indefinitely, and therefore the step density on the facet vanishes in the long-time scaling limit. Moreover, in Appendix C we show that in the long-time limit, the step density is a continuous function even at the facet edge; i.e., it goes to zero continuously as the facet edge is approached from above.

Denoting the scaled position of the facet edge by x_0, the above observations can be expressed in the form

$$F(x)=0,\quad \forall x\leqslant x_0. \tag{33}$$

Note that $F(x)=0$ is not a solution of Eq. (28). This does not contradict the continuum model, since the model was derived only for the case of a finite step density [see Eq. (22)]. Thus the scaling function has to satisfy Eq. (28) only at $x>x_0$, and $x=x_0$ is a *singular* point.

Let us now study the nature of this singularity at the facet edge. Returning to our simulation data, we note that near the facet edge, the scaling function is extremely steep (see Fig. 3). Indeed, the expansion of Eq. (28) in small F suggests that in the vicinity of x_0, $F(x)$ can be written as a power series in $\sqrt{x-x_0}$. Thus although F is continuous at x_0, all its derivatives with respect to x diverge at the singular point.

We now turn to discuss the boundary conditions necessary to solve Eq. (28). First, we examine the behavior of F at infinity. Far enough from the origin the steps do not move. Hence in the limit $\rho\to\infty$ the step density remains at its initial value. This implies that

$$\lim_{x\to\infty}F(x)=1. \tag{34}$$

It turns out that this condition corresponds to two boundary conditions, since it is only possible to satisfy Eq. (34) if F' vanishes at infinity. In fact, by considering the asymptotic expansion of F, it can be shown that for large x

$$F=1+a_4x^{-4}+O(x^{-8}), \tag{35}$$

where $a_4=3(1+g)$ in the DL case and $a_4=\frac{3}{2}(1+g)$ in the ADL case.

In order to solve Eq. (28), we need two additional boundary conditions at $x=x_0$. The first of these is $F(x_0)=0$ [see Eq. (33)]. Another boundary condition at $x=x_0$ can be derived by enforcing volume conservation. From Eq. (15), the volume change during the time τ is given by

$$2\pi\int_0^\infty \rho[h(\rho,\tau)-h(\rho,0)]d\rho. \tag{36}$$

Integrating this equation by parts and requiring volume conservation, we get

$$\int_0^\infty \rho^2[D(\rho,\tau)-D(\rho,0)]d\rho=0. \tag{37}$$

In terms of scaled variables, the preceding equation can be written as

$$\int_0^\infty x^2(F-1)dx=\int_{x_0}^\infty x^2(F-1)dx-\frac{x_0^3}{3}=0, \tag{38}$$

where we have used the fact that F vanishes below x_0. The evaluation of the integral in Eq. (38) can be done by multiplying Eq. (28) by x^2 and integrating it with respect to x. The resulting equation is

$$\int_{x_0}^\infty x^2\left(\frac{F'\mathcal{A}}{2}+F^2\mathcal{B}\right)dx=\int_{x_0}^\infty \frac{x^3F'}{4}dx. \tag{39}$$

The integral $\mathcal{M}_2=\int x^2(F'\mathcal{A}/2+F^2\mathcal{B})dx$ on the left-hand side is carried out in Appendix C, and is expressed in terms of F and its derivatives. The result of this integration combined with integration by parts of the right-hand side of Eq. (39) leads to

$$\int_{x_0}^\infty x^2(F-1)dx=\frac{1}{3}[x^3(F-1)-4\mathcal{M}_2]\Big|_{x_0}^\infty. \tag{40}$$

Inserting this relation in Eq. (38), we obtain the boundary condition

$$\mathcal{M}_2|_{x_0}=0. \tag{41}$$

We have used the facts that the surface term at infinity in Eq. (40) vanishes and $F(x_0)=0$.

At this point we have four boundary conditions, two at infinity and two at x_0. We may now obtain a unique solution of Eq. (28) if we know the value of x_0. What determines x_0? To answer this question, consider the height of the cone at the origin, h_0, at time $\tau=\tau_{n-1}$ and at time $\tau=\tau_n$. τ_{n-1} and τ_n are the disappearance times of two successive steps, and therefore $h_0(\tau_{n-1})-h_0(\tau_n)=1$. We can also calculate this difference from Eq. (14). Combining these two results, we arrive at the relation

$$(\tau_n^{1/\gamma}-\tau_{n-1}^{1/\gamma})\int_0^\infty (F-1)dx=-1. \tag{42}$$

Recalling that $\tau_n=(\theta_0 n)^\gamma$ and using the fact that F vanishes below x_0, we can rewrite the preceding equation as

$$\int_{x_0}^\infty (F-1)dx-x_0=-\theta_0^{-1}. \tag{43}$$

The integral in Eq. (43) can be evaluated by integrating Eq. (28) with respect to x. The result is

$$\int_{x_0}^\infty (F-1)dx=4\mathcal{M}_0|_{x_0}+x_0, \tag{44}$$

where the integral $\mathcal{M}_0=\int(F'\mathcal{A}/2+F^2\mathcal{B})dx$ is carried out in Appendix C and is expressed in terms of F and its derivatives. Combining Eq. (43) and Eq. (44), we obtain the relation

$$4\mathcal{M}_0|_{x_0}=-\theta_0^{-1}. \tag{45}$$

The left-hand side of this equation depends on x_0, thus relating x_0 to θ_0, the scaled collapse time period of the steps. What then is the value of θ_0? It is determined by the motion and collapse of the first step. The behavior of the first step is different from that of all the other steps, since it does not have neighboring steps with smaller radii. Thus, our continuum model, which treats all the steps on equal footing, does not contain any information on the value of θ_0. We therefore expect *a family* of valid scaling functions consistent with the continuum model with different values of x_0 or θ_0. The unique value of x_0 observed in simulations is determined by the discrete nature of the steps, and at this stage we are not able to calculate it.

VI. NUMERICAL EVALUATION OF THE SCALING FUNCTION

We now find the scaling function numerically. Consider first the DL case. We choose a value of x_0 and solve Eq. (28) starting at $x=x_0$. As explained in the preceding section, F can be expanded in powers of $\sqrt{x-x_0}$ in the vicinity of x_0:

$$F(x)=\sum_{n=1}^\infty k_n(\sqrt{x-x_0})^n, \tag{46}$$

where we have already used the boundary condition (33). We therefore have three additional free parameters in this expansion, which should be determined by the boundary conditions (34) and (41). We choose these parameters as the first three odd coefficients in the expansion (46): k_1, k_3, and k_5 (the first two even coefficients vanish). Using the boundary condition (41), we can express k_5 as a function of k_1 and k_3 through the relation

$$k_5=\frac{k_1}{6x_0^2}-\frac{k_3^2}{2k_1}+\frac{k_3}{9x_0}-\frac{1}{6gx_0^3k_1},$$

thus reducing the number of free parameters to two.

Finally we use the boundary condition (34) to find the coefficients k_1 and k_3. Since Eq. (34) addresses the value of F at infinity, it cannot be easily applied to the expansion of F in the vicinity of x_0. We therefore start from an initial guess for the values of k_1 and k_3, solve Eq. (28) numerically for this choice of parameters, and then tune k_1 and k_3 until the boundary condition (34) is satisfied. For a given choice of k_1 and k_3, we found the solution of Eq. (28) in the following way. Numerical integration starting at x_0 is impossible because the derivatives of F diverge there. Therefore, we first used the expansion (46), truncated at a high enough order, to

evaluate the function F and its first three derivatives at $x = x_0 + \delta x$, for some choice of δx. Then, using these values we integrated Eq. (28) numerically from $x_0 + \delta x$. We made sure that the solution is not sensitive to the choice of δx.

The above procedure was employed to generate the scaling function for a range of values of the scaled facet edge position, x_0, and the following picture emerged. There is a special minimal value of x_0, which we denote by x_0^*. For $x_0 < x_0^*$, there is no solution of Eq. (28) which satisfies the boundary conditions. For each value of $x_0 \geq x_0^*$, there is a unique solution which satisfies the boundary conditions. Thus, as we anticipated, there is a one-dimensional family of scaling functions parametrized by the value of $x_0 \geq x_0^*$.

Since x_0 is related to θ_0 through Eq. (45), this family of solutions can alternatively be labeled by the value of θ_0. We used Eq. (45) to calculate $\theta_0(x_0)$ and found that it is a monotonically decreasing function. In particular, $\theta_0(x_0)$ is maximal at x_0^*. This is reasonable, since it means that a smaller facet corresponds to a longer period and thus to a slower facet edge.

Despite the existence of many possible scaling functions, our simulations suggest that the system reaches a unique scaling solution independent of initial conditions. What is the selected solution? In Fig. 6 we compare the calculated scaling functions with simulation data in the DL case. We do this for three different values of g, the interaction strength parameter. When g is large, there is an impressive agreement between the simulations data and the x_0^* solution [Fig. 6(a)]. When g is reduced (i.e., for weaker interactions between steps) the observed scaling function deviates from the x_0^* solution [Figs. 6(b) and 6(c)]. However, in these cases there is another solution with a larger value of x_0 that best fits the simulation data. The agreement between this best-fit solution and the simulation data is again excellent.

The above observations suggest that x_0^* is the selected solution in the large g limit. We propose the following argument to support this scenario. Since the parameter g is a measure of the strength of the step-step interaction G relative to the step line tension Γ, the large g limit is equivalent to the small Γ limit. The collapse of the first step is driven by the step line tension. In the large g limit, the collapse driving force is minimal and the collapse time period is maximal. As we mentioned above, a long collapse period is equivalent to a large value of θ_0, which corresponds to a small value of x_0. Thus the large g limit corresponds to the minimal value of x_0, i.e., $x = x_0^*$.

Now consider the ADL case. Although in this limit we can also expand F in $\sqrt{x - x_0}$, the numerical procedure described above is not an effective method of solution in this case. It turns out that the resulting scaling functions are sensitive to the choice of δx. We therefore had to use a different method to solve Eq. (28) in the ADL case. Let us denote by x_{peak} the minimal value of x, which corresponds to a local maximum of F. Such a point must exist for any continuous function satisfying the integral condition (38) and the boundary conditions (33) and (34). By tuning the values of $F(x_{\mathrm{peak}})$, $F''(x_{\mathrm{peak}})$, and $F'''(x_{\mathrm{peak}})$ we found a one-dimensional family of scaling functions, which satisfy the boundary conditions. This family can be parametrized by the value of the x_{peak} or alternatively by the value of the resulting

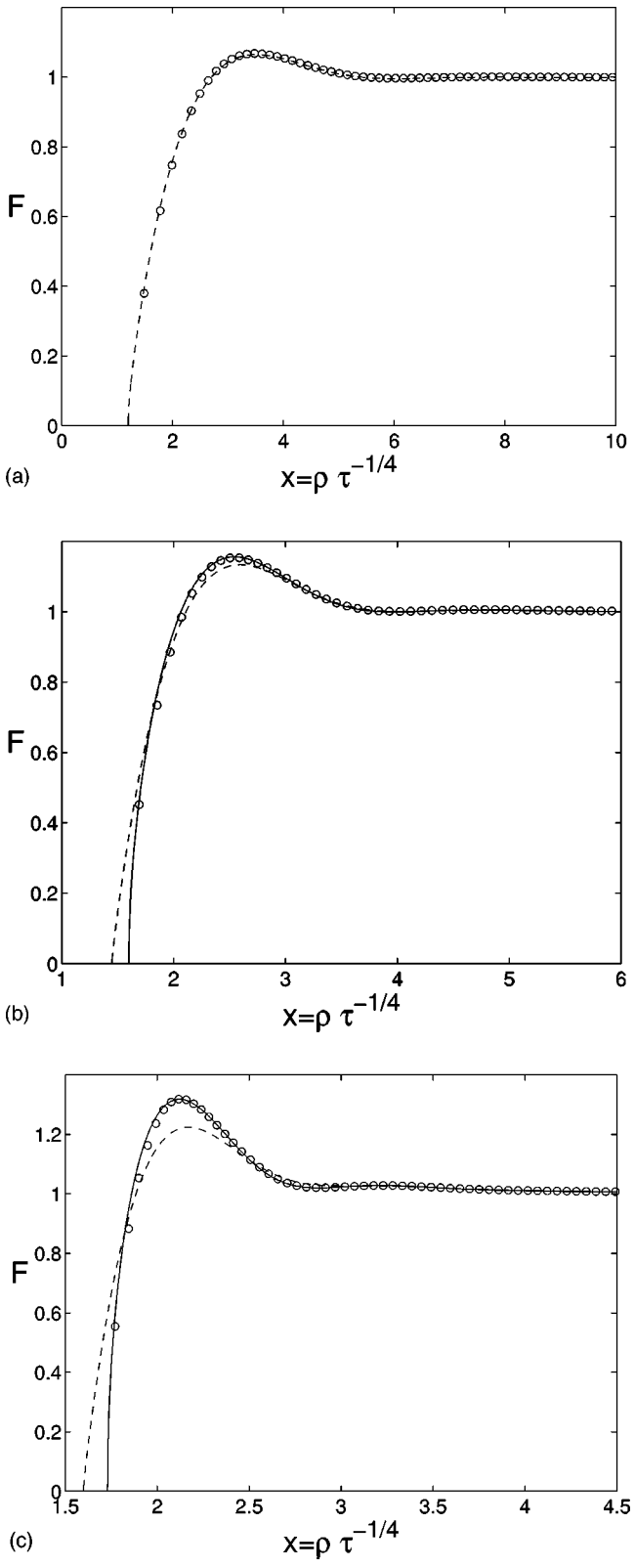

FIG. 6. Numerical solutions for the DL scaling function compared with simulation data. Results for three different values of the step-step interaction parameter are shown: (a) $g = 0.1$, (b) $g = 0.01$, and (c) $g = 0.001$. When the step-step interaction is strong, the x_0^* solution (dashed line) agrees very well with the simulation data (circles). As the value of g is reduced, the best-fit solution of Eq. (28) (solid) deviates from the x_0^* solution to higher values of x_0.

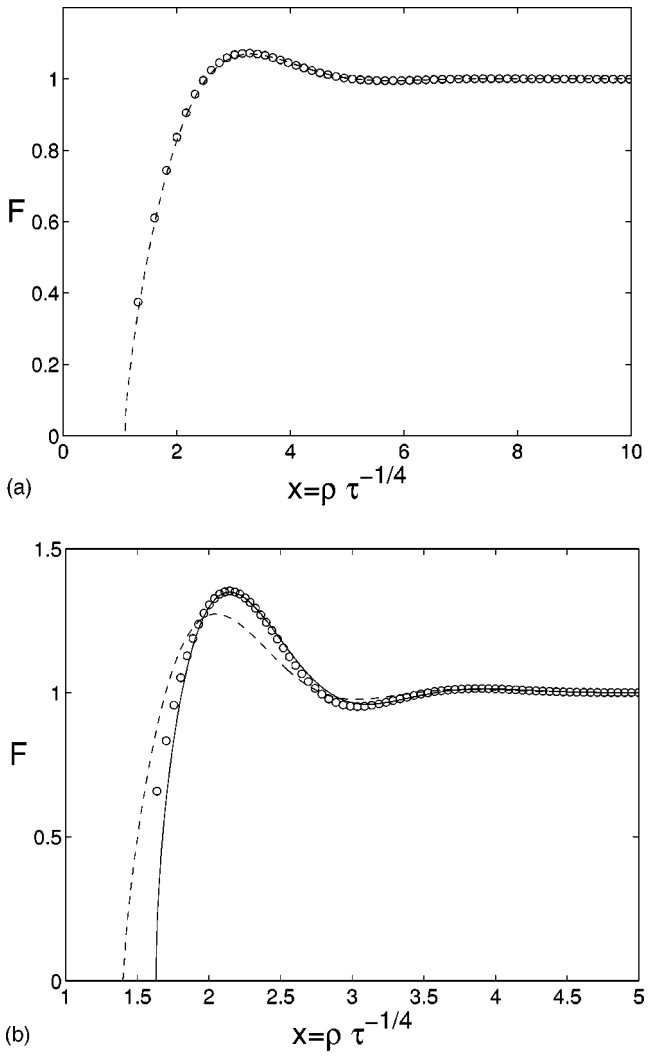

FIG. 7. Numerical solutions for the ADL scaling function compared with simulation data. Results for two different values of the step-step interaction parameter are shown: (a) $g=0.2$ and (b) $g=0.01$. When the step-step interaction is strong, the simulation data (circles) agree with the $x_0^*=1.09\pm0.07$ solution (dashed line). As g is reduced, we notice that the best-fit solution of Eq. (28) (solid line) deviates from the $x_0^*=1.4\pm0.07$ solution to higher values of x_0.

x_0. As in the DL case, we find that there is a minimal value of x_0, denoted by x_0^*, below which there are no solutions satisfying the boundary conditions.

Figure 7 shows the simulation data compared with calculated scaling functions for two values of the interaction strength g. We again find that for large g the simulation data agree with the x_0^* solution (dashed line). When g is reduced, the agreement deteriorates and there is a different solution with $x_0>x_0^*$ (solid line) which best fits the simulation data.

VII. EFFECTS OF STEP PERMEABILITY

The step-flow model we introduced in Sec. II assumes that steps are impermeable; i.e., adatoms cannot hop between neighboring terraces without being incorporated in the step separating them. In general, however, steps may be permeable. For example, in a recent paper,[16] Tanaka *et al.* interpret their experimental results as evidence that steps on Si(001) are permeable. We therefore ask the following question: What is the effect of step permeability on decay of nanostructures in general, and on the decay of an infinite cone in particular? In this section we show that the scaling exponents of an infinite cone of permeable steps are identical to the exponents associated with impermeable steps. Moreover, the only effect of step permeability on the differential equation for the scaling function is a renormalization of one of its parameters.

Following Ref. 16, we generalize our step-flow model to include step permeability. We assume that flux of adatoms between two neighboring terraces due to direct hops is determined by first-order kinetics. Introducing the permeability coefficient p, we rewrite Eq. (3) as

$$D_s\left.\frac{\partial C_i}{\partial r}\right|_{r_i}=k(C_i|_{r_i}-C_i^{\mathrm{eq}})+p(C_i|_{r_i}-C_{i-1}|_{r_i}),$$
$$-D_s\left.\frac{\partial C_{i-1}}{\partial r}\right|_{r_i}=k(C_{i-1}|_{r_i}-C_i^{\mathrm{eq}})-p(C_i|_{r_i}-C_{i-1}|_{r_i}). \tag{47}$$

Step permeability does not affect the diffusion equation itself, and therefore the general form of the diffusion field, given by Eq. (2), remains unaltered. However the coefficients A_i and B_i are affected, and the equations for coefficients of different terraces become coupled. As a result, the step equations of motion cannot be written in closed form. The scaling analysis therefore becomes more cumbersome.

As in the case of impermeable steps, we assume that in the long-time limit the scaling ansatz Eq. (11) holds, with the same definitions of the scaled variables, x and θ in terms of ρ and τ. We slightly change the definition of the dimensionless time τ to $\tau=t/t_0$, where t_0 is a time scale which we can choose to our convenience. The derivation of the exponents α and β in Sec. IV did not involve the dynamics of the system. Thus the same derivation still holds and the values of α and β are not affected by step permeability. We proceed to evaluate the exponent γ and the scaling function F by studying Eq. (47).

For convenience, we parametrize the solutions of the diffusion equation by concentration differences instead of the parameters A_i and B_i. These concentration differences, U_i and V_i, are defined as follows:

$$U_i=C_i(r_i)-\overline{C}^{\mathrm{eq}}=A_i\ln r_i+B_i-\overline{C}^{\mathrm{eq}},$$
$$V_i=C_i(r_i)-C_i(r_{i+1})=A_i\ln\frac{r_i}{r_{i+1}}. \tag{48}$$

In the continuum limit, U_i and V_i are continuous functions of r and t or alternatively of x and θ. We associate the values of U_i and V_i with the middle of the ith terrace, namely

$$U\left(\frac{x_i+x_{i+1}}{2},\theta\right)=U_i,$$
$$V\left(\frac{x_i+x_{i+1}}{2},\theta\right)=V_i. \tag{49}$$

The scaling scenario for the functions U and V is

$$U(x,\theta)=\theta^{\mu}[u(x)+O(\theta^{-1})],$$
$$V(x,\theta)=\theta^{\nu}[v(x)+O(\theta^{-1})]. \tag{50}$$

In terms of U_i, V_i, and the dimensionless radii ρ_i, Eq. (47) takes the form

$$\frac{TD_sV_i}{\Omega\Gamma\rho_i\ln\frac{\rho_i}{\rho_{i+1}}}=k(U_i-\overline{C}^{\rm eq}\xi_i)+p[U_i-(U_{i-1}-V_{i-1})], \tag{51}$$

$$-\frac{TD_sV_{i-1}}{\Omega\Gamma\rho_i\ln\frac{\rho_{i-1}}{\rho_i}}=k(U_{i-1}-V_{i-1}-\overline{C}^{eq}\xi_i)-p[U_i-(U_{i-1}-V_{i-1})].$$

Evaluating Eq. (51) at $x=(x_i+x_{i+1})/2$ we can now employ Eq. (24) to expand ξ_i, $\rho_i\ln(\rho_i/\rho_{i+1})$ and $\rho_i\ln(\rho_{i-1}/\rho_i)$ in powers of θ^{-1}:

$$\xi_i=\left[\frac{1}{x}+g\left(\frac{F^2}{x}+3FF'\right)\right]\theta^{-1}+O(\theta^{-2}),$$
$$\rho_i\ln\frac{\rho_i}{\rho_{i+1}}=-\frac{1}{F}+O(\theta^{-1}), \tag{52}$$
$$\rho_i\ln\frac{\rho_{i-1}}{\rho_i}=-\frac{1}{F}+O(\theta^{-1}).$$

The x_i's dependence of U and V is unknown, so we expand

$$u\left(\frac{x_{i-1}+x_i}{2}\right)=\sum_{n=0}^{\infty}\frac{1}{n!}\frac{\partial^n u(x)}{\partial x^n}\left(\frac{x_{i-1}+x_i}{2}-x\right)^n,$$
$$v\left(\frac{x_{i-1}+x_i}{2}\right)=\sum_{n=0}^{\infty}\frac{1}{n!}\frac{\partial^n v(x)}{\partial x^n}\left(\frac{x_{i-1}+x_i}{2}-x\right)^n. \tag{53}$$

Since the difference between successive x's is of order θ^{-1}, Eq. (53) is also an expansion in this small parameter.

Using Eq. (53) together with Eqs. (49) and (50) we isolate $v(x)$ in Eqs. (51), keeping only the lowest orders in θ^{-1},

$$\theta^{1+\nu}v(x)=-\frac{\Omega\Gamma k\left\{\theta^{1+\mu}u(x)-\overline{C}^{\rm eq}\left[\frac{1}{x}+g\left(\frac{F^2}{x}+3FF'\right)\right]\right\}}{D_sTF+p\Omega\Gamma},$$
$$\theta^{1+\nu}v(x)=\frac{\Omega\Gamma k\left\{\theta^{1+\mu}u(x)-\overline{C}^{\rm eq}\left[\frac{1}{x}+g\left(\frac{F^2}{x}+3FF'\right)\right]\right\}}{D_sTF+(p+k)\Omega\Gamma}. \tag{54}$$

Since $v(x)$ cannot vanish identically, the two expressions above are consistent only if $\nu<-1$, $\mu=-1$, and

$$u(x)=\overline{C}^{\rm eq}\left[\frac{1}{x}+g\left(\frac{F^2}{x}+3FF'\right)\right]. \tag{55}$$

Thus, both sides of Eqs. (54) decay in time. We now subtract the second line of Eq. (51) from the first line and obtain the following equation:

$$\frac{D_sT}{\Omega\Gamma}\left(\frac{V_{i-1}}{\rho_i\ln\frac{\rho_{i-1}}{\rho_i}}+\frac{V_i}{\rho_i\ln\frac{\rho_i}{\rho_{i+1}}}\right)=(k+2p)(U_i-U_{i-1}+V_{i-1}). \tag{56}$$

Again we expand to lowest order in θ^{-1} and isolate $v(x)$:

$$v(x)=-\theta^{-(2+\nu)}\frac{\Omega\Gamma(k+2p)}{2D_sTF^2+\Omega\Gamma(k+2p)F}u'(x). \tag{57}$$

$v(x)$ does not depend on θ. This implies that $\nu=-2$ and $v(x)$ is proportional to $u'(x)$.

To finish the scaling analysis, we return to Eq. (21) and find the leading orders in θ^{-1} of $\dot{\rho}_{i+1}+\dot{\rho}_i$ and $\dot{\rho}_{i+1}-\dot{\rho}_i$. Using Eqs. (5) and (48), we find that

$$\dot{\rho}_i=\frac{D_sT^2}{\Omega\Gamma^2}t_0\left(\frac{V_i}{\rho_i\ln\frac{\rho_i}{\rho_{i+1}}}-\frac{V_{i-1}}{\rho_i\ln\frac{\rho_{i-1}}{\rho_i}}\right). \tag{58}$$

Putting together Eqs. (50), (52), and (58) we conclude that to lowest order in θ^{-1},

$$\dot{\rho}_{i+1}+\dot{\rho}_i=\theta^{-3}[\mathcal{A}_p+O(\theta^{-1})],$$
$$\dot{\rho}_{i+1}-\dot{\rho}_i=\theta^{-4}[\mathcal{B}_p+O(\theta^{-1})]. \tag{59}$$

$\mathcal{A}_p$ and $\mathcal{B}_p$ are expressions involving F, F', F'', F''', and F''''. Note that the orders of θ^{-1} in these expressions are identical to those in the equivalent expressions in Sec. IV [Eq. (25)]. These orders are responsible for the result $\gamma=4$ in the case of impermeable steps. Therefore, in the permeable case we also have $\gamma=4$.

After expanding $\dot{\rho}_{i+1}+\dot{\rho}_i$ and $\dot{\rho}_{i+1}-\dot{\rho}_i$, we can use Eq. (21) to obtain the differential equation for the scaling function in the permeable case. However, this exercise is not necessary. We avoid it by arguing that the resulting differential equation in the permeable case is equivalent to the one in the impermeable case with renormalization of some of the parameters. To see this, we note that the treatment we presented here is valid also in the impermeable case. Thus when $p=0$, the general differential equation must be equivalent to the equation derived in Sec. IV. In addition, the attachment/detachment rate k and the permeability p affect the step velocities only through the function $v(x)$, which depends on k and p only through the sum $k+2p$. Therefore, k and p affect the differential equation itself only through the sum $k+2p$. We conclude that the scaling function in the case of permeable steps is identical to the scaling function of impermeable steps with $k+2p$ in the former replacing k in the latter.

VIII. SUMMARY AND DISCUSSION

We have studied the relaxation of an infinite crystalline cone below the roughening temperature, in terms of a step-flow model. The model was solved numerically and two types of dynamical evolutions were found. When the repul-

sive interactions are strong enough, the decay of the cone proceeds through the collapse of the innermost steps, one step at a time. Weak interactions lead to a step-bunching instability (except in pure diffusion limited kinetics), and the decay process becomes much more complicated and involves collapse of bunches of steps.

Focusing on stable cases, we found that in the long-time limit the decaying step system obeys a scaling scenario. The step density (i.e., the slope of the height profile), defined as the inverse step separation, scales in time according to $D(\rho,\tau)=\tau^{\alpha/\gamma}F(\tau^{-\beta/\gamma}\rho,\tau^{1/\gamma})$. F is a function of the scaled position $x=\tau^{-\beta/\gamma}\rho$ and exhibits a periodic dependence on the scaled time $\theta=\tau^{1/\gamma}$. In particular, the position of the facet edge at the top of the cone grows as $\tau^{\beta/\gamma}$. The values of the scaling exponents which fit our simulations are $\alpha=0$, $\beta=1$, and $\gamma=4$.

Following this observation we used a scaling ansatz to transform the discrete step-flow model into a continuum description of surface evolution. The basic predictions of this continuum model are the values of the scaling exponents (which agree with the simulation results) and a differential equation for the scaling function F. This continuum model becomes exact in the long-time scaling limit, and it breaks down whenever the step density vanishes. This fact can be seen both from the derivation of the continuum model and from the resulting differential equation, which predicts a singular behavior at the zeros of the scaling function F.

We showed that each physical solution of the continuum equation has a special point, x_0, at which the scaling function, F, vanishes. F is singular at $x=x_0$, and we identify this special point as the scaled position of a facet edge. Thus the edge of a macroscopic facet in the discrete system is a singular point of the scaling function F.

A detailed analysis of the discrete system revealed a sufficient number of boundary conditions, which define a unique scaling function, F, for a given value of the scaled facet edge position, x_0. However, we were not able to find a unique value for x_0, and were left with a one-dimensional family of solutions, parametrized by x_0. A numerical solution of the differential equation for F confirmed the existence of this family. We found that there is a minimal value of x_0, which we denoted by x_0^*. For every $x_0 \geqslant x_0^*$, there is a unique scaling function, while for $x_0 < x_0^*$ there are no solutions which satisfy the boundary conditions.

A comparison of the numerical solutions of F with results of simulations of the discrete system leads to the following picture. When the step-step repulsion is strong, there is a remarkable agreement between the $x_0=x_0^*$ solution and the simulation data. When the magnitude of the step-step interaction is reduced, the system reaches scaling solutions with $x_0>x_0^*$. We therefore advance the hypothesis that in the strong interaction limit the system approaches the minimal x_0^* solution.

Although our work provides a detailed account of the decay process of an infinite cone, it leaves a few unresolved issues. First and most important is the fact that we were not able to uniquely determine the value of x_0. We did show that x_0 depends crucially on the detailed collapse process of the innermost step, which is not included in the continuum model. Thus, in order to evaluate x_0, one has to deal directly with the discrete step system. Another open issue related to the behavior of the innermost step is the periodic behavior of the scaling function. This periodicity is observed in the kinetics of the discrete system of steps, and is absent from the solution of the continuum equation. Lastly, when the repulsive interaction between steps is weaker than a certain threshold, the system becomes unstable and step bunches are formed. The critical value of the interaction below which this instability occurs and its dependence on the kinetic parameter q have not been studied so far. We intend to address these open questions in future work.

Finally, we remark that the scaling behavior of the cone profile, predicted in this work, is robust, in particular the existence of a facet growing as $\tau^{1/4}$, as well the existence of a scaling state does not depend on the detailed form of the repulsive interactions between steps. A quantitative change of these interactions may alter the scaling function, F, but the scaling exponents do not change. Another manifestation of the robustness of the scaling solution is the effect of step permeability. In principle, step permeability could have changed the scaling behavior of the system entirely. However, we showed that its only effect on the scaling solution is to modify the attachment-detachment rate coefficient, k, to $k+2p$.

ACKNOWLEDGMENTS

We are grateful to N. Bartelt, H. C. Jeong, D. J. Liu, and J. D. Weeks for helpful discussions. This research was supported by Grant No. 95-00268 from the United States–Israel Binational Science Foundation (BSF), Jerusalem, Israel.

APPENDIX A

Here we study the linear stability of circular, uniformly spaced steps with unit-step separation in the absence of step-step interactions. This configuration with $\rho_n=n$ is not a steady state. However, in the large radius limit the steps move very slowly, and the uniform state is extremely close to a steady state. We therefore refer to it as a quasisteady state. We regard the quasisteady state as unstable if the growth of perturbations is faster than the motion of steps.

In the absence of step-step interactions, Eqs. (10) simplify to

$$\dot{\rho}_n \equiv \frac{d\rho_n}{d\tau} = \frac{a_n - a_{n-1}}{\rho_n}, \tag{A1}$$

with

$$a_n = \frac{\dfrac{1}{\rho_n} - \dfrac{1}{\rho_{n+1}}}{(1-q)\ln\dfrac{\rho_n}{\rho_{n+1}} - q\left(\dfrac{1}{\rho_n} + \dfrac{1}{\rho_{n+1}}\right)}. \tag{A2}$$

For large values of n, the velocity of the nth step in the quasisteady state is given by

$$\dot{\rho}_n = \frac{n^{-3}}{1+q} + O(n^{-4}). \tag{A3}$$

To check the linear stability of the above configuration, we perturb the step positions according to

$$\rho_n = n + \Delta e^{i(\phi n - \omega t)}. \tag{A4}$$

Equating the time derivative of this perturbation with the velocity of the nth step results in an equation for ω. We find that to the lowest orders in Δ and n^{-1},

$$\omega = \frac{4iq(1-\cos\phi)n^{-2}}{(1+q)^2}. \tag{A5}$$

Since the magnitude of ω is significantly larger than the step velocities in the quasisteady state, positive values of $\mathrm{Im}(\omega)$ lead to an instability. We see that away from the DL case ($q>0$) the system is unstable. The most unstable mode is $\phi=-\pi$ (step pairing). The $\phi=0$ mode (uniform translation) is marginal as is the $q=0$ (DL) case.

APPENDIX B

In this appendix we give some technical details of the algebraic manipulations performed in Secs. IV and V.

To calculate expressions $\mathcal{A}$ and $\mathcal{B}$ in Eq. (25), we first express the scaled positions of the steps as power series in θ^{-1}. Inserting Eq. (24) into Eq. (23) we find that to fifth order in θ^{-1}

$$x_{i-2} = x - \frac{5\theta^{-1}}{2F} - \frac{3F'\theta^{-2}}{F^3} + \frac{5(-3F'^2+FF'')\theta^{-3}}{2F^5} + \frac{(-93F'^3+61FF'F''-6F^2F^{(3)})\theta^{-4}}{4F^7}$$
$$- \frac{[1935F'^4-1890FF'^2F''+260F^2F'F^{(3)}+F^2(180F''^2-17FF^{(4)})]\theta^{-5}}{24F^9},$$

$$x_{i-1} = x - \frac{3\theta^{-1}}{2F} - \frac{F'\theta^{-2}}{F^3} + \frac{(-3F'^2+FF'')\theta^{-3}}{2F^5} - \frac{(33F'^3-21FF'F''+2F^2F^{(3)})\theta^{-4}}{12F^7}$$
$$+ \frac{(-135F'^4+126FF'^2F''-12F^2F''^2-16F^2F'F^{(3)}+F^3F^{(4)})\theta^{-5}}{24F^9},$$

$$x_i = x - \frac{\theta^{-1}}{2F},$$

$$x_{i+1} = x + \frac{\theta^{-1}}{2F},$$

$$x_{i+2} = x + \frac{3\theta^{-1}}{2F} - \frac{F'\theta^{-2}}{F^3} - \frac{(-3F'^2+FF'')\theta^{-3}}{2F^5} - \frac{(33F'^3-21FF'F''+2F^2F^{(3)})\theta^{-4}}{12F^7}$$
$$- \frac{(-135F'^4+126FF'^2F''-12F^2F''^2-16F^2F'F^{(3)}+F^3F^{(4)})\theta^{-5}}{24F^9},$$

$$x_{i+3} = x + \frac{5\theta^{-1}}{2F} - \frac{3F'\theta^{-2}}{F^3} - \frac{5(-3F'^2+FF'')\theta^{-3}}{2F^5} + \frac{(-93F'^3+61FF'F''-6F^2F^{(3)})\theta^{-4}}{4F^7}$$
$$+ \frac{[1935F'^4-1890FF'^2F''+260F^2F'F^{(3)}+F^2(180F''^2-17FF^{(4)})]\theta^{-5}}{24F^9}, \tag{B1}$$

where F and its derivatives are evaluated at $x=(x_i+x_{i+1})/2$.

Using these expressions we expand the step velocities in θ^{-1} and obtain Eq. (25). In the general case the expressions for $\mathcal{A}$ and $\mathcal{B}$ are too cumbersome to be written here. Instead we give these expressions in the two limiting cases. In the DL case,

$$\mathcal{A}_{\mathrm{DL}} = g\left(\frac{2F}{x^3} - \frac{4F'}{x^2} + \frac{10F'^2}{Fx} + \frac{10F''}{x} + \frac{18F'F''}{F} + 6F^{(3)}\right)$$
$$+ \frac{2}{Fx^3},$$

$$\mathcal{B}_{\mathrm{DL}}=g\left(-\frac{3}{x^4}+\frac{5F'}{Fx^3}-\frac{5F'^3}{F^3x}-\frac{7F''}{Fx^2}+\frac{10F'F''}{F^2x}+\frac{9F''^2}{F^2}-\frac{F'^2(5F+9x^2F'')}{F^3x^2}+\frac{5F^{(3)}}{Fx}+\frac{9F'F^{(3)}}{F^2}+\frac{3F^{(4)}}{F}\right)-\frac{3}{F^2x^4}-\frac{F'}{F^3x^3}. \tag{B2}$$

Inserting Eq. (B2) into Eq. (28) we find the differential equation which governs the scaling function in the DL case:

$$g\left(12F'F^{(3)}+3FF^{(4)}+9F''^2+\frac{15F'F''+5FF^{(3)}}{x}-\frac{7(F'^2+FF'')}{x^2}+\frac{6FF'}{x^3}-\frac{3F^2}{x^4}\right)-\frac{3}{x^4}-\frac{xF'}{4}=0. \tag{B3}$$

In the ADL case,

$$\mathcal{A}_{\mathrm{ADL}}=g\left(\frac{1}{x^3}-\frac{F'}{Fx^2}+\frac{3F'^2}{F^2x}-\frac{3F'^3}{F^3}+\frac{5F''}{Fx}+\frac{6F'F''}{F^2}+\frac{3F^{(3)}}{F}\right)+\frac{1}{F^2x^3}+\frac{F'}{F^3x^2},$$

$$\mathcal{B}_{\mathrm{ADL}}=g\left(-\frac{3}{2Fx^4}+\frac{F'}{F^2x^3}-\frac{F'^2}{F^3x^2}-\frac{3F'^3}{F^4x}+\frac{9F'^4}{2F^5}-\frac{3F''}{F^2x^2}+\frac{F'F''}{2F^3x}-\frac{21F'^2F''}{2F^4}+\frac{3F''^2}{F^3}+\frac{5F^{(3)}}{2F^2x}+\frac{3F'F^{(3)}}{2F^3}+\frac{3F^{(4)}}{2F^2}\right)-\frac{3}{2F^3x^4}-\frac{2F'}{F^4x^3}-\frac{3F'^2}{2F^5x^2}+\frac{F''}{2F^4x^2}, \tag{B4}$$

and the differential equation for the ADL scaling function is

$$g\left(-\frac{3F}{2x^4}+\frac{3F'}{2x^3}-\frac{3F'^2}{2Fx^2}-\frac{3F'^3}{2F^2x}+\frac{3F'^4}{F^3}-\frac{3F''}{x^2}+\frac{3F'F''}{Fx}-\frac{15F'^2F''}{2F^2}+\frac{3F''^2}{F}+\frac{5F^{(3)}}{2x}+\frac{3F'F^{(3)}}{F}+\frac{3F^{(4)}}{2}\right)-\frac{3}{2Fx^4}-\frac{3F'}{2F^2x^3}-\frac{xF'}{4}-\frac{F'^2}{F^3x^2}+\frac{F''}{2F^2x^2}=0. \tag{B5}$$

In Sec. V we used the moments

$$\mathcal{M}_0=\int\left(\frac{F'\mathcal{A}}{2}+F^2\mathcal{B}\right)dx,$$

$$\mathcal{M}_2=\int x^2\left(\frac{F'\mathcal{A}}{2}+F^2\mathcal{B}\right)dx$$

to set boundary conditions for the scaling function at x_0.

In the DL case,

$$\mathcal{M}_{0_{\mathrm{DL}}}=g\left(\frac{F^2}{x^3}-\frac{2FF'}{x^2}+\frac{5F'^2}{x}+\frac{5FF''}{x}+9F'F''+3FF'''\right)+\frac{1}{x^3},$$

$$\mathcal{M}_{2_{\mathrm{DL}}}=g\left(\frac{3F^2}{x}-6FF'-xF'^2-xFF''+9x^2F'F''+3x^2FF'''\right)+\frac{3}{x}.$$

In the ADL case,

$$\mathcal{M}_{0_{\mathrm{ADL}}}=g\left(\frac{F}{2x^3}-\frac{F'}{2x^2}+\frac{3F'^2}{2xF}-\frac{3F'^3}{2F^2}+\frac{5F''}{2x}+\frac{3F'F''}{F}+\frac{3F'''}{2}\right)+\frac{1}{2x^3F}+\frac{F'}{2x^2F^2},$$

$$\mathcal{M}_{2_{\mathrm{ADL}}}=g\left(\frac{3F}{2x}-\frac{5F'}{2}-\frac{3xF'^2}{2F}-\frac{3x^2F'^3}{2F^2}-\frac{xF''}{2}+\frac{3x^2F'F''}{F}+\frac{3x^2F'''}{2}\right)+\frac{3}{2xF}+\frac{F'}{2F^2}.$$

APPENDIX C

In this appendix we show that in the scaling state, the step density near the facet edge must vanish when the facet size diverges. This implies that $F(x_0)=0$, where x_0 is the scaled position of the facet edge. We restrict ourselves to situations where steps collapse towards the origin one at a time (consistently with simulation results).

It is tempting to argue that since our system is expanding and slowing down, in the long-time limit it approaches the equilibrium state of straight steps in contact with a facet. In this equilibrium state the step density near the facet edge vanishes as a square root. This equilibrium state is not consistent with our density function, which also predicts a square root approach to zero, but with a time-dependent coefficient. Moreover, even in the long-time limit, steps in our system continue to collapse. In each collapse period, just before the step disappears, its chemical potential diverges. At these times the system is not close to equilibrium.

Consider the velocity of the first step. It depends on the positions of the first three steps ρ_1, ρ_2, and ρ_3 through

$$\dot{\rho}_1=\frac{1}{\rho_1}\frac{\xi_1-\xi_2}{(1-q)\ln\frac{\rho_1}{\rho_2}-q\left(\frac{1}{\rho_1}+\frac{1}{\rho_2}\right)}. \tag{C1}$$

ρ_2 is always larger than ρ_1, so the denominator is always negative. The direction of motion of the first step is thus given by the sign of the numerator,

$$\mathcal{N}=\xi_1-\xi_2=\frac{1}{\rho_1}-\frac{1}{\rho_2}+2g\left(\frac{1}{(\rho_2-\rho_1)^3}-\frac{\rho_3}{\rho_2+\rho_3}\frac{1}{(\rho_3-\rho_2)^3}\right), \tag{C2}$$

which must be positive to avoid bounding of the first and second steps.

Fixing ρ_2 and ρ_3, the value of ρ_1^* which minimizes $\mathcal{N}$ is found by solving

$$\left.\frac{\partial\mathcal{N}}{\partial\rho_1}\right|_{\rho_1^*}=\frac{6g}{(\rho_2-\rho_1^*)^4}-\frac{1}{\rho_1^{*2}}=0. \tag{C3}$$

The only solution between ρ_2 and the origin is

$$\rho_1^*=\rho_2+\sqrt{\frac{3g}{2}}-\sqrt{\rho_2\sqrt{6g}+\frac{3g}{2}}.$$

This is indeed a minimum since the second derivative of $\mathcal{N}$ with respect to ρ_1 is always positive when $0\leqslant\rho_1\leqslant\rho_2$.

Substituting ρ_1^* into $\mathcal{N}$, we find that

$$\mathcal{N}(\rho_1^*)=\frac{1}{\rho_2+\sqrt{\frac{3g}{2}}-\sqrt{\rho_2\sqrt{6g}+\frac{3g}{2}}}-\frac{1}{\rho_2}+\frac{2g}{\left(\sqrt{\rho_2\sqrt{6g}+\frac{3g}{2}}-\sqrt{\frac{3g}{2}}\right)^3}-\frac{2g\rho_3}{(\rho_2+\rho_3)(\rho_3-\rho_2)^3}. \tag{C4}$$

The first three terms of $\mathcal{N}(\rho_1^*)$ decay when ρ_2 is large. The fourth term, however, will remain finite unless the difference $\rho_3-\rho_2$ diverges with ρ_2. If the fourth term does remain finite, $\mathcal{N}(\rho_1^*)$ becomes negative, the velocity of the first step becomes positive, and the first step cannot pass ρ_1^* on its way to the origin.

The above analysis indicates that the step density vanishes near the facet edge. We consider two scenarios for the collapse of the first step. In the first scenario the step starts the collapse from a position below ρ_1^*. In this case the separation between the first and second steps is initially divergent since $\rho_2-\rho_1^*$ diverges as $\sqrt{\rho_2}$. But the initial configuration in the collapse of one step is the final configuration of the former collapse period. Thus the former period ended with a divergent distance $\rho_3-\rho_2$.

In the second scenario the first step starts to collapse from a position above ρ_1^*. If the first step collapses alone (i.e., ρ_2 is large throughout the collapse period), the distance $\rho_3-\rho_2$ must grow to allow ρ_1 to pass through ρ_1^*.

Either way there must be some point in the collapse period where the separation $\rho_3-\rho_2$ diverges. At this point the step density near the facet edge vanishes.

*Electronic address: israeli@wicc.weizmann.ac.il
†Electronic address: fekandel@wicc.weizmann.ac.il

[1] S. Tanaka, C. C. Umbach, J. M. Blakely, R. M. Tromp, and M. Mankos, J. Vac. Sci. Technol. A **15**, 1345 (1997); *Structure and Evolution of Surfaces*, edited by R. C. Cammarata, E. H. Chason, T. L. Einstein, and E. D. Williams, Materials Research Society Symposia Proceedings No. 440 (MRS, Pittsburgh, 1997), p. 25.
[2] J. Blakely, C. Umbach, and S. Tanaka, *Dynamics of Crystal Surface and Interfaces*, edited by P. M. Duxbury and T. J. Pence (Plenum, New York, 1997), p. 23.
[3] C. C. Umbach, M. E. Keeffe, and J. M. Blakely, J. Vac. Sci. Technol. A **9**, 1014 (1991).
[4] K. Yamashita, H. P. Bonzel, and H. Ibach, Appl. Phys. **25**, 231 (1981).
[5] W. W. Mullins, J. Appl. Phys. **28**, 333 (1957); **30**, 77 (1959).
[6] H. P. Bonzel and W. W. Mullins, Surf. Sci. **350**, 285 (1996).
[7] H. P. Bonzel and E. Preuss, Surf. Sci. **336**, 209 (1995); Appl. Phys. A: Solids Surf. **35**, 1 (1984).
[8] J. Hager and H. Spohn, Surf. Sci. **324**, 365 (1995).
[9] F. Lancon and J. Villain, Phys. Rev. Lett. **64**, 293 (1990).
[10] M. Ozdemir and A. Zangwill, Phys. Rev. B **42**, 5013 (1990).
[11] M. V. Ramana Murty and B. H. Cooper, Phys. Rev. B **54**, 10 377 (1996). These Monte Carlo simulations agree with Refs. 15 and 10.
[12] M. A. Dubson and G. Jeffers, Phys. Rev. B **49**, 8347 (1994).
[13] Z. Jiang and C. Ebner, Phys. Rev. B **40**, 316 (1989).
[14] J. D. Erlebacher and M. J. Aziz, Surf. Sci. **374**, 427 (1997). These Monte Carlo simulations agree with Ref. 15 and disagree with Ref. 10.
[15] A. Rettori and J. Villain, J. Phys. (France) **49**, 257 (1988).
[16] S. Tanaka, N. C. Bartelt, C. C. Umbach, R. M. Tromp, and J. M. Blakely, Phys. Rev. Lett. **78**, 3342 (1997).
[17] C. Duport, A. Chame, W. W. Mullins, and J. Villain, J. Phys. I **6**, 1095 (1996).
[18] E. Adam, A. Chame, F. Lancon, and J. Villain, J. Phys. I **7**, 1455 (1997).
[19] E. S. Fu, M. D. Johnson, D. J. Liu, J. D. Weeks, and E. D. Williams, Phys. Rev. Lett. **77**, 1091 (1996).
[20] K. Morgenstern, G. Rosenfeld, and G. Comsa, Phys. Rev. Lett. **76**, 2113 (1996).
[21] M. Uwaha, J. Phys. Soc. Jpn. **57**, 1681 (1988).
[22] J. Villain, Europhys. Lett. **2**, 531 (1986).
[23] W. Selke and P. M. Duxbury, Phys. Rev. B **52**, 17 468 (1995).
[24] W. K. Burton, N. Cabrera, and F. C. Frank, Philos. Trans. R. Soc.

London, Ser. A **243**, 299 (1951).
[25] N. Israeli and D. Kandel, Phys. Rev. Lett. **80**, 3300 (1998).
[26] G. S. Bales and A. Zangwill, Phys. Rev. B **41**, 5500 (1990).
[27] V. I. Marchenko and A. Ya. Parshin, Zh. Éksp. Teor. Fiz. **79**, 257 (1980) [Sov. Phys. JETP **52**, 129 (1980)].
[28] A. F. Andreev and Yu. A. Kosevich, Zh. Éksp. Teor. Fiz. **82**, 1435 (1981) [Sov. Phys. JETP **54**, 761 (1981)].
[29] P. Nozières, J. Phys. I **48**, 1605 (1987).